Novel hierarchical SnO_2 microsphere catalyst coated on gas diffusion electrode for enhancing energy efficiency of CO_2 reduction to formate fuel

Fu, Yishu; Li, Yanyan; Liu, Yuyu; Qiao, Jinli; Zhang, Jiujun; Wilkinson, David P.

Publisher's version / Version de l'éditeur:
https://doi.org/10.1016/j.apenergy.2016.03.115
Applied Energy, 175, pp. 536-544, 2016-04-05

Applied Energy xxx (2016) xxx–xxx

Contents lists available at ScienceDirect

Applied Energy

journal homepage: www.elsevier.com/locate/apenergy

Novel hierarchical SnO_2 microsphere catalyst coated on gas diffusion electrode for enhancing energy efficiency of CO_2 reduction to formate fuel

Yishu Fu [a], Yanan Li [a], Xia Zhang [a], Yuyu Liu [b,d,*], Jinli Qiao [a,*], Jiujun Zhang [b,c], David P. Wilkinson [c]

[a] College of Environmental Science and Engineering, Donghua University, 2999 Ren'min North Road, Shanghai 201620, China
[b] Institute for Sustainable Energy Storage and Conversion, Shanghai University (SU-ISESC), Shanghai 200444, China
[c] Department of Chemical and Biochemical Engineering, Vancouver, BC, Canada
[d] Multidisciplinary Research on the Circulation of Waste Resources, Graduate School of Environmental Studies, Tohoku University, Aramaki, aza Aoba 6-6-20, Aoba-ku, Sendai 980-8579, Japan

HIGHLIGHTS

- HMS-SnO_2/GDE was developed for electrocatalytic reduction of CO_2 to formate fuel.
- The influence of ethanol/H_2O ratio on selectivity and activity was studied by electrochemical characterization.
- A faradaic efficiency of 62.0% in a divided H-type two-compartment cell was observed at −1.7 V.
- The HMS-SnO_2/GDE electrode was stable over 12 h of continuous electrolysis operation.

GRAPHICAL ABSTRACT

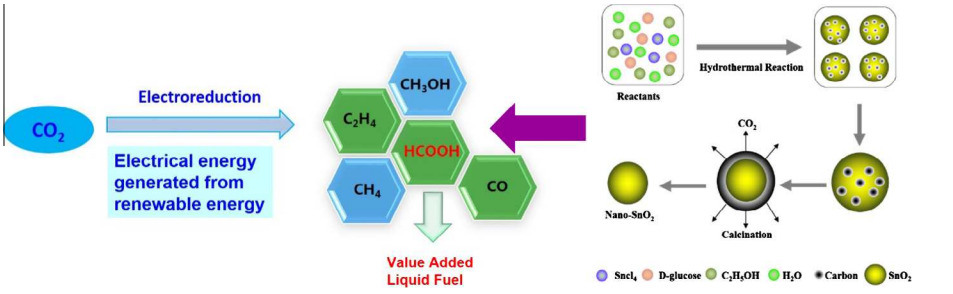

ARTICLE INFO

Article history:
Received 19 January 2016
Received in revised form 29 February 2016
Accepted 28 March 2016
Available online xxxx

Keywords:
Electrochemical CO_2 reduction
Micro/nano-SnO_2 particles
Formate
Faradaic efficiency
Electrode stability

ABSTRACT

The conversion of carbon dioxide to value-added fuel using electrical energy generated intermittently from renewable energy sources is very promising in terms of energy usage reconciliation. The process converts greenhouse carbon dioxide gas to produce diverse attractive chemicals and fuels like methanol, formate, and other hydrocarbons. In this paper, the electroreduction of CO_2 to formate in aqueous solution is performed by using novel hierarchical tin oxide microsphere (HMS-SnO_2) particles deposited over gas diffusion layer electrode (HMS-SnO_2/GDE). The experiment is carried out in a divided H-type two-compartment cell with a Nafion® membrane as the diaphragm separating the cathodic and anodic compartments. The HMS-SnO_2 catalysts are synthesized by a facile hydrothermal self-assembled process using different ratios of ethanol to distilled water in the synthetic solution. Due to the outstanding catalytic activity and selectivity toward CO_2 electroreduction, SnO_2-86/GDE exhibits a high Faradaic efficiency of 62% toward formate formation at −1.7 V vs. SHE (Standard Hydrogen Electrode). The electrode durability is also observed with a stable current density over 12 h of continuous electrolysis operation. The superior performance is credited to the morphology- and size-controlled hierarchical structure, which may provide more active sites to accelerate the slow kinetics of CO_2 reduction, leading to the improved energy efficiency. During electrolysis process, $KHCO_3$ electrolyte is found to have some contribution to formate formation on the micro-structured tin oxide catalysts coated GDE electrode.

* Corresponding authors at: Institute for Sustainable Energy Storage and Conversion, Shanghai University (SU-ISESC), Shanghai 200444, China (Y. Liu). College of Environmental Science and Engineering, Donghua University, 2999 Ren'min North Road, Shanghai 201620, China (J. Qiao).
E-mail addresses: liu@mail.kankyo.tohoku.ac.jp (Y. Liu), qiaojl@dhu.edu.cn (J. Qiao).

http://dx.doi.org/10.1016/j.apenergy.2016.03.115
0306-2619/

1. Introduction

The emission of carbon dioxide (CO_2) due to human activities has produced extra content in the atmosphere, leading to the carbon unbalance of Earth, probably resulting in negative impact on our environment through global warming. For overcoming this negative effect, several important approaches to reduce CO_2 emission, such as carbon capture/sequestration (CCS) and CO_2 conversion into useful low-carbon fuels, have been carried out in the most recent years [1]. As one of the approaches, CO_2 conversion to useful fuels seems to be a more attractive and promising option in terms of both increasing energy efficiency and environmental protection. Among various CO_2 conversion techniques, the electrochemical conversion using intermittent electricity generated from renewable energy sources has been considered one of the most feasible and innovative techniques, which can not only reduce CO_2, but also produce diverse valuable fuels including formic acid, carbon monoxide, methanol, oxalic acid and hydrocarbons [2–6]. Production of useful value-added chemicals, like ethanol from CO_2 as an alternative to petrochemistry appears promising as it has a double advantage of reusing CO_2 while sparing fossil resources and avoiding CO_2 emissions from their use [7]. The process requires little energy input compared to their respective market values. However, due to both the extreme sluggish kinetics of CO_2 electroreduction and low reaction selectivity, the reduction process necessitates the use of specific metal catalysts [8]. For example, in aqueous solution, one of the main products is formic acid with high Faradaic efficiency if *sp*-group metals such as Hg, In, Sn and Pb based catalysts are employed [9].

Tin (Sn)-based materials have been considered to be promising electrocatalysts for CO_2 reduction to produce small fuels (e.g. formate, methanol or hydrocarbons) because of their low cost, wide availability and reasonable overall Faradaic efficiency [10]. Normally, the Sn metal based electrodes could also have high selectivity in the production of formate in aqueous electrolytes. This is particularly attractive because the formate can be used as a fuel for direct formate fuel cells [11] and also as the optimal hydrogen carrier [12]. Currently the formate is produced by hydrolysis of methyl formate and hydrolysis of formamide, with negative environmental impact and relative expensive production costs. Developing an efficient electrocatalytic process for formate production could reduce the costs and enhance its use in fuel cells and related applications [13]. These formate products may thus offset costs associated with carbon management. Besides, the introduction of such carbonaceous products to markets might significantly improve the world economy by lowering production costs of several intermediates, providing massive and cheap production of some final products [7]. However, as realized, the deactivation of Sn metal based electrodes during CO_2 reduction is very fast, and the reduction reaction on these electrodes requires at least ~860 mV of overpotential at a current density of 4–5 mA cm^{-2} in an aqueous solution saturated with 1 atm CO_2 [14]. To overcome these challenges, several approaches have been explored using different structures of Sn-based electrodes, such as Sn particles (shots and granules), Sn foil, or Sn-based gas diffusion electrodes [15–20].

Most recently, Chen and Kanan [21] reported a SnO_x/Sn composite electrode could participate in the CO_2 reduction pathway by providing chemical functionality that might stabilize the incipient negative charge on CO_2 (i.e., CO_2^-) or by mediating the electron transfer directly, therefore the Faradaic efficiency of ~58% for formate formation was obtained on such a SnO_x/Sn electrode, which was much higher than that of ~19% observed on pure Sn foil electrode. Zhou et al. [10] found that if the electrode was only composed of SnO_2 layer with a thickness of ~3.5 nm, the highest Faradaic efficiency (64%) towards formate formation could be observed at −1.2 V. Due to the controlled structure and morphology, the metal/metal oxides nanoparticle surfaces may provide abundant undercoordinated sites, which are more likely to be the active sites for CO_2 reduction [22–24]. All above previous works reported single Sn metal or SnO_x/Sn electrode, which suggested the application of SnO_x on CO_2 electroreduction showed very interesting and promising results. This insight has indicated that SnO_x catalyst exhibits greatly enhanced CO_2 reduction activity relative to a typical Sn electrode. Furthermore, as this material is stable in most organic and aqueous solutions, it is a promising candidate for CO_2 electroreduction.

In this work, the operation of a continuous electroreduction process of CO_2 to formate in aqueous solutions is studied by using electrodes with hierarchical tin oxide microsphere (HMS-SnO_2), which are a new series of morphology and size controlled HMS-SnO_2 catalysts with high catalytic efficiency for CO_2 electroreduction. The catalyst structures are induced by a facile hydrothermal self-assembled process through changing different ratios of ethanol to distilled water in the synthetic solution. The advantages of this synthesis method are a decrease in the electrochemical potential at which electrochemical reductions occur and an increase in the selectivity of the process. To maximize surface area, all the synthesized SnO_2 microsphere catalysts are coated on the gas diffusion layer (GDL) to form 3D porous structures for facilitating the mass transportation from the gas–liquid interface to the catalyst surface [25–27]. In this way, easy diffusion path lengths can be achieved for substrates to access, leading to faster kinetics. Furthermore, the evolution of byproduct H_2, which could impede the reduction reaction between CO_2 and electrode, could also be inhibited effectively [28]. Therefore, the aim of this work is to study the electrode (SnO_2 coated on the GDL) morphology and size effects on catalytic activity, product selectivity, Faradaic efficiency and energy efficiency. It is also studied systematically using techniques such as cyclic voltammetry, linear sweep voltammetry, and ion chromatography. Electrochemical measurements show the catalysts can have outstanding catalytic activity, selectivity and good stability toward CO_2 electroreduction. These electrochemical tests can help to provide a more detailed understanding of the process and the influence of these parameters on the resulting reactivity. During CO_2 reduction process, catalysts hold the key to successful industrial applications. Therefore, this work could effectively increase the number of industrial applications by improving the CO_2 electroreduction reactions for commercialization and should be an integral part of research and development for carbon management and sustainable development.

In our work, with 1–3 μm large SnO_2 microspheres composed of sub-structured nanoparticles (20–40 nm), a maximum Faradaic efficiency of >62% for formate production is achieved. These catalysts are very stable during electrolysis and can continue producing formate for at least 12 h. Possible catalytic mechanism for these SnO_2 nanoparticle coated electrodes is discussed based on the measurements and analysis of scanning electron microscopy, crystal-phase X-ray diffraction pattern, high-resolution transmission electron microscopy and selected area electron diffraction analyses, as well as X-ray photoelectron spectroscopy. For further understanding, the chemical compositions of the electrode materials before and after a long time electrolysis are also analyzed. In addition, the effect of $KHCO_3$ electrolyte on the CO_2 reduction is also investigated using both the N_2-saturated $KHCO_3$ solution and CO_2-saturated pure H_2O for comparison.

2. Experimental

2.1. Catalyst synthesis

The SnO_2 microsphere catalysts were synthesized by a facile hydrothermal self-assembled process, where $SnCl_4$ and D-glucose

Please cite this article in press as: Fu Y et al. Novel hierarchical SnO_2 microsphere catalyst coated on gas diffusion electrode for enhancing energy efficiency of CO_2 reduction to formate fuel. Appl Energy (2016), http://dx.doi.org/10.1016/j.apenergy.2016.03.115

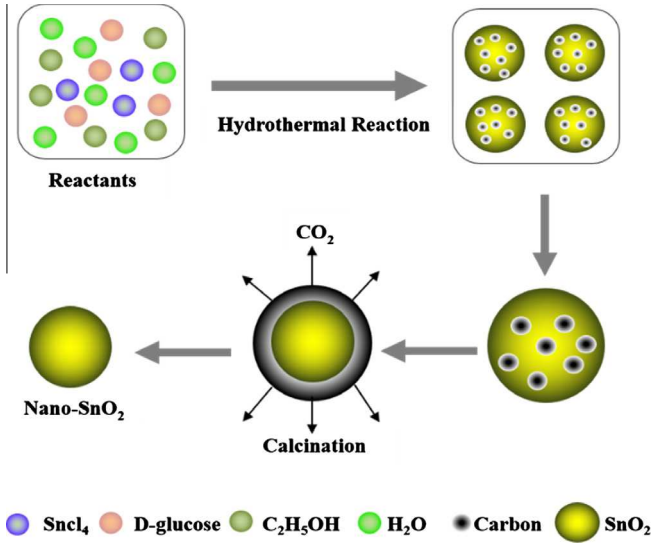

Scheme 1. Representative illustration of the formation of HMS-SnO_2 in solvothermal synthesis.

monohydrate were used as the precursors, as illustrated in Scheme 1. For a typical synthesis, 4 mmol of $SnCl_4$ and 10 mmol of D-glucose monohydrate were dissolved in a mixture of distilled water and ethanol (35 mL) under stirring till forming a transparent colorless solution. Then this mixture solution was transferred into a 100 mL Teflon-lined stainless steel autoclave, which was sealed and maintained at 180 °C for 24 h before it was cooled down in air. The sediment with a black color was collected and washed by ethanol/water several times, and was dried in a vacuum oven at 60 °C for 5 h. The final powder was calcined at 550 °C for 5 h in air, during which the black sediment was gradually turned into a white one, indicating the successful removal of carbon by oxidization in air. In this way, the SnO_2 microspheres with controlled size and morphology were obtained just by changing the volume ratio of ethanol to distilled water as shown in Fig. 1 (30:5) and Fig. 3 ((a) 10.5:24.5, (b) 24.5:10.5, (c) 30:5, (d) 35:0).

2.2. Electrode preparation and electrochemical test

For working electrode preparation, the SnO_2 microsphere catalysts synthesized above were used to prepare catalyst inks which were then coated onto the carbon paper sheet (CPS) (Toray, TGP-H-090) to form gas diffusion electrodes (GDEs). In a typical preparation, as-prepared SnO_2 catalyst (3 mg cm^{-2} loading) was dispersed in a mixture of 100 mg of 5 wt.% Nafion solution and 1.4 mL of 99.7 wt.% isopropyl alcohol (Sinopharm Chemical Reagent Co.) to form catalyst ink [29], which was then coated on CPS (4 cm^2) to form a SnO_2 microsphere catalyst coated gas-diffusion electrode (abbreviated as SnO_2/GDE).

For electrochemical characterization, a standard H-type cell (Aldrich Nafion®117) equipped with both gas inlet and outlet, which allow the passage of either N_2 (99.99%) or CO_2 (99.99%) through the solution, was used for measuring both catalyst property and CO_2 reduction performance. In the measurements, SnO_2/GDE was used as the working electrode and a piece of Nafion®117 cation exchange membrane (H^+ form) as a separator, platinum foil electrode as the counter electrode and a saturated calomel electrode (SCE) as the reference electrode, respectively. Prior to all experiments, the solution was purged with N_2 for at least 30 min to remove all dissolved air. For CO_2 reduction measurements, the solution was bubbled with 1.0 atm CO_2 gas (99.99%) for 30 min before measurements. All electrochemical measurement was performed on a CH Instrument 660E.

The electrocatalytic activity and kinetics of SnO_2/GDE working electrode were tested using both cyclic voltammetry (CV) and linear sweep voltammetry (LSV) at scan rates of 50 mV s^{-1} and 5 mV s^{-1}, respectively, and in a potential range of 1.0∼−1.6 V vs. SCE. The controlled potential electrolysis was carried out using a CHI660E electrochemical analyzer in the same standard H-type cell. Before each electrolysis process, the electrolyte was bubbled with CO_2 for at least 30 min, and CO_2 gas was continuously

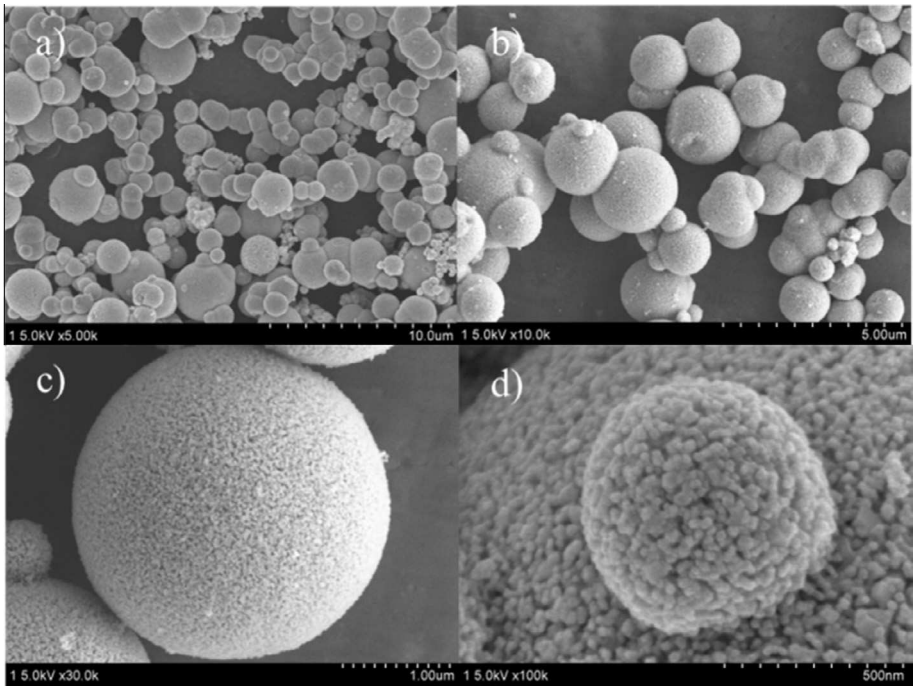

Fig. 1. SEM images of HMS-SnO_2 aggregates at different magnifications, i.e., (a) (×5000), (b) (×10,000), (c) (×30,000), and (d) (×100,000). The synthetic solution with ethanol/water ratio to be 30:5.

Please cite this article in press as: Fu Y et al. Novel hierarchical SnO_2 microsphere catalyst coated on gas diffusion electrode for enhancing energy efficiency of CO_2 reduction to formate fuel. Appl Energy (2016), http://dx.doi.org/10.1016/j.apenergy.2016.03.115

bubbled to maintain the saturation during the following electrolysis. For the potentiostatic measurements, a constant potential of −1.70 V vs. SHE was imposed for 12 h for stability test, where the electrolysis current was continuously recorded. For soluble product measurements, the electrolysis time was controlled for 60 min. All these tests were carried out at ambient temperature and pressure.

2.3. Physical characterization and product analysis

The morphology of as-prepared SnO_2 microsphere catalysts was characterized by Zeiss ultra plus thermal field emission SEM instrument (Carl Zeiss SMTAG, Germany). The crystal-phase X-ray diffraction (XRD) patterns of SnO_2 catalysts were obtained using a Philips PW3830 X-ray diffractometer equipped with Cu Ka radiation (λ = 0.15406 nm). The intensity data was collected at 25 °C in the 2 range from 0° to 90° with a scan rate of 1.20 min^{-1}. High-resolution transmission electron microscopy (HR-TEM) and selected area electron diffraction (SAED) analyses were performed with a high-resolution Hitachi JEM-2100F operating at 200 kV to obtain the information of the average particle size and the crystal properties of catalysts. For chemical composition measurement after long time electrolysis, the SnO_2 microsphere catalysts were analyzed by the X-ray photoelectron spectroscopy (XPS) measurements on a Kratos AXIS UltraDLD electron spectrometer with Al K X-ray anode source ($h\upsilon$ = 1486.6 eV) at 250 W and 14.0 kV. For the analysis of the reduction soluble products, before product measurements, the solution after CO_2 reduction was diluted 50 times or 100 times (which is convenient to formate being detected in mobile phase), then it was filtered with filter membrane (0.22 μm) and the products in the electrolyte were directly analyzed by ion chromatography (ICS-90, Dionex, USA) using an AS144 mm × 250 mm separation column at a flow rate of 1 mL/min. In this analysis, the mobile phase was a mixed aqueous solution of Na_2CO_3 (3.5 mM) and $NaHCO_3$ (1.0 mM), and a H_2SO_4 (20 mM) aqueous solution was used as a regenerative liquid.

3. Results and discussion

3.1. Surface structure of SnO_2 microsphere catalysts

As typical catalyst sample, Fig. 1(a)–(c) shows three different magnifications of SEM images of SnO_2-86 catalyst, which was prepared using a synthetic solution with ethanol/water ratio of 30:5. It can be observed that the SnO_2-86 catalyst shows a clear and uniform sphere-like structure with 1–3 μm in overall dimension (Fig. 1a and b). The high magnification SEM image of Fig. 1c indicates a large sphere size in diameter of 3 μm. Further from the high magnification SEM image as indicated by Fig. 1d, one spherical particle of 680 nm can be clearly observed which parasitized on large microsphere particle surface. All these large spherical particles indicate a clear 3-dimensioned hierarchical structure, which are comprised of the secondary structures entirely by aggregated small primary SnO_2 nanoparticles in the size of 20–40 nm in diameter. This special morphology structure may greatly influences the catalytic activity of the catalysts for CO_2 electroreduction, which would be demonstrated in the following section.

The formation mechanism can be described as schematically illustrated in Scheme 1. In order to determine the dominating factors in the process, a series of experiments were carried out to understand the formation of SnO_2 nanoparticle aggregates. The interesting microstructure of an as-synthesized large hierarchical microsphere SnO_2 (HMS-SnO_2) can be further corroborated by TEM images, as displayed in Fig. 2a and b. In agreement with the above SEM observations (Fig. 1c and d), a high uniformity of the microspheres can be seen from the TEM images. A high-magnification TEM image of nanoparticles further shows the microcosmic characteristics of microsphere SnO_2 as shown in Fig. 2c. The nanoparticles display a similar polygon structure of approximately 20–40 nm. The TEM bright-field imaging combined with selected-area electron diffraction (SAED) reveals the fine microstructure of the HMS-SnO_2, each wire being a monocrystal with a tetragonal rutile structure, as shown in Fig. 2d [30]. The corresponding ring-like SAED pattern (Fig. 2d) indicates the nanostructures are crystalline, and the diffraction rings from inside to outside can be indexed to (110), (200), (211), (202), (103) and (223) planes of SnO_2 nanocrystals with hexagonal symmetry, respectively. High-resolution (HR) imaging was combined with SAED to investigate the nanoparticles growth direction. As shown in Fig. 2e, the HR-TEM image of nanoparticles shows a clear shape similar to a polygon structure. Fig. 2f further shows a high-magnification image of HR-TEM, indicating that the nanoparticles are exposed two growth directions of (110) and (101) facets. Fourier transforms (FFTs) of the HR-TEM image (insets) show three facets, (110), (101) and (200), which are in accordance with the XRD results (Fig. S1). Meanwhile, the FFTs combined with macroscopic XRD further confirms the rutile structure.

In order to determine the key factors in the microsphere synthesis, the volume ratio of ethanol to distilled water were changed to ascertain the formation of SnO_2 nanoparticles aggregates. It is found the ethanol/water ratio plays an important role in the formation of microspheres morphology. Fig. 3(a)–(d) shows the SEM images of SnO_2 as-prepared from different ratios of ethanol to distilled water as solvent, i.e., SnO_2-30 and SnO_2-70, SnO_2-86 and SnO_2-100, respectively. Fig. 3a shows that when the ratio is 30%, only a plane composed of some tight SnO_2 nanoparticles could be formed, as can be seen in the insert image of Fig. 3(a). When the ethanol content in the mixed solvent is increased to 70% (i.e., SnO_2-70), the morphology of SnO_2 begins to change largely to some microspheric aggregates (Fig. 3b), the size of SnO_2 particles is increased dramatically up to 1–1.5 μm with a large microsphere structure. However, there still exists numerous microspheres accumulated. The distinguishable HMS-SnO_2 particles can only be produced when the ethanol content is larger than 80% (i.e., SnO_2-86 and SnO_2-100) (Fig. 3c and d). However, in a pure ethanol solution (i.e., SnO_2-100), the interior of the microsphere structures begins to collapse and becomes small aggregated nanoparticle of ca. 20–30 nm, which is formed surrounding the SnO_2 microsphere (Fig. 3d).

The crystallinity and phase purity of as-prepared SnO_2 aggregates are independently confirmed by XRD (Fig. S1(a–d)). All the peaks in the XRD pattern in Fig. S1 could be indexed to crystalline SnO_2 by comparing with JCPDS card No. 41–1445, indicating it has good phase purity, and the crystalline SnO_2 nanoparticles are small in size. All SnO_2 aggregates have the similar diffractions, although SnO_2-86 sample shows four additional small peaks (Fig. S1(c)). In comparison with other SnO_2 samples, the SnO_2-86 sample has a well-defined morphology of hierarchical microsphere structure, as shown in Fig. 1c and d, which may be responsible for these additional four peaks. It can also be seen the crystallinity of all SnO_2 aggregates becomes pronounced as indicated by the increased intensities of the four diffraction peaks of (110), (101), (200) and (211), which can be assigned to tetragonal SnO_2. The main diffraction (110), (101), (200), and (211) peaks are relatively broad, indicating that the nanoparticles are composed of SnO_2 nano-crystalline. The crystallinity can be calculated to be 71.7% and the crystalline grain sizes of these four crystal surfaces are 14.8, 17.1, 15.4 and 15.7 nm, respectively. A panoramic view reveals that SnO_2-86 is entirely consist of uniform microspheres without impurity particles or aggregates, as clearly observed in the SEM images (Fig. 1).

Please cite this article in press as: Fu Y et al. Novel hierarchical SnO_2 microsphere catalyst coated on gas diffusion electrode for enhancing energy efficiency of CO_2 reduction to formate fuel. Appl Energy (2016), http://dx.doi.org/10.1016/j.apenergy.2016.03.115

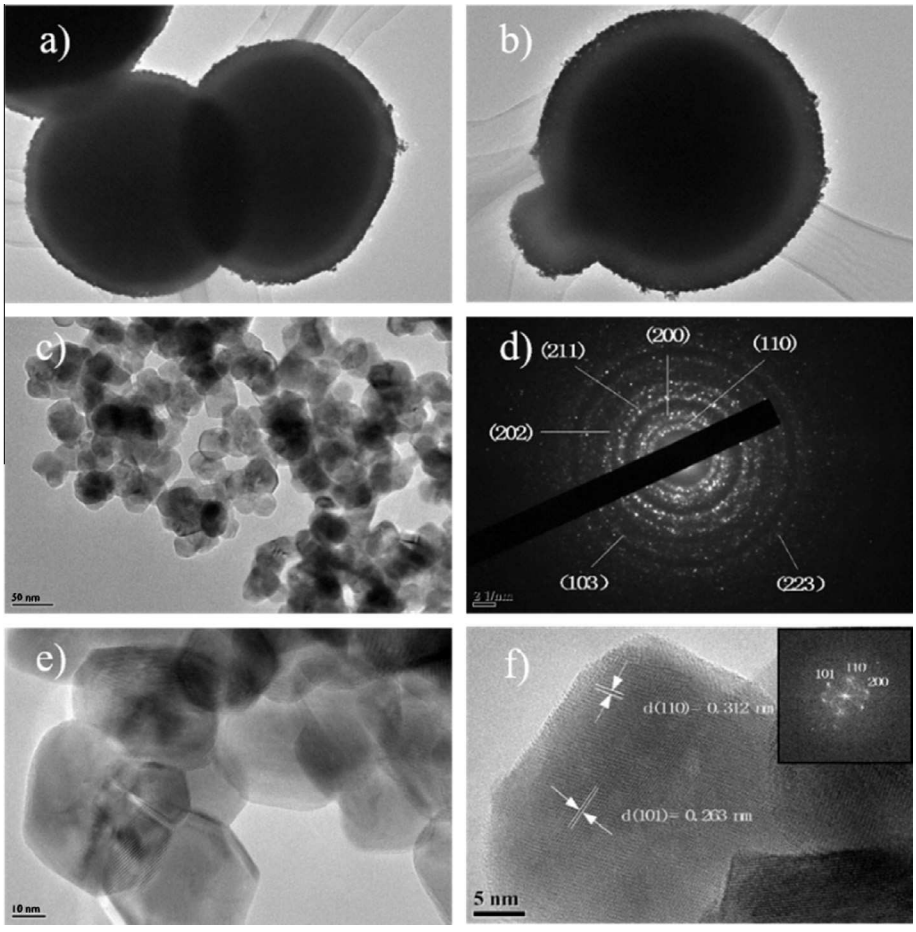

Fig. 2. (a, b) Low-magnification TEM images of as-prepared HMS-SnO_2, (c, e, f) Enlarged TEM images of HMS-SnO_2 at different magnifications with (f) insert FFT pattern, (d) The selected area electron diffraction pattern (SAED) of HMS-SnO_2. The synthetic solution with ethanol/water ratio to be 30:5.

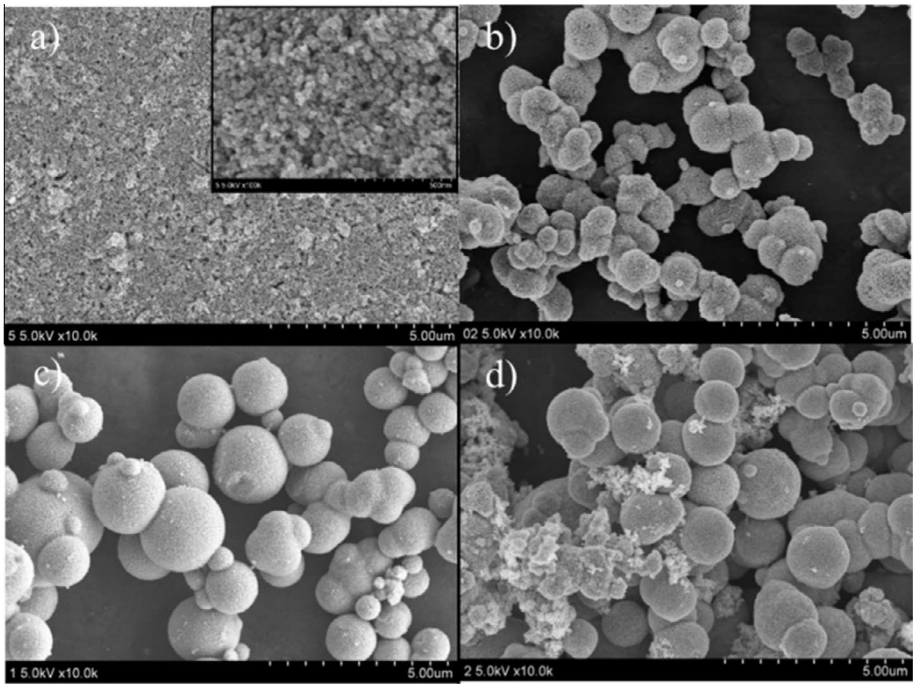

Fig. 3. SEM images of solvothermal products prepared from different ratios of ethanol to distilled water as solvent. (a) SnO_2-30, (b) SnO_2-70, (c) SnO_2-86 and (d) SnO_2-100, respectively.

Please cite this article in press as: Fu Y et al. Novel hierarchical SnO_2 microsphere catalyst coated on gas diffusion electrode for enhancing energy efficiency of CO_2 reduction to formate fuel. Appl Energy (2016), http://dx.doi.org/10.1016/j.apenergy.2016.03.115

3.2. Electrocatalytic performance toward CO_2 reduction

To evaluate the CO_2 reduction activity of the HMS-SnO_2 electrode prepared from SnO_2/GDE-86, cyclic voltammetric (CV) measurements were carried out in both N_2- and CO_2-saturated 0.5 M $KHCO_3$ solution, separately, as shown in Fig. 4a. The anodic peaks between −0.3 V and −0.8 V and the cathodic peak between −0.7 V and −1.0 V in CV curves can be attributed to the formation and reduction of tin oxides in basic media, respectively [31]. The SnO_2/GDE-86 electrode exhibits a less negative onset potential at −0.48 V vs. SHE, which is 100 mV more positive than that of under N_2. At a high overpotential of −1.36 V, a sharp increase in the current densities can be observed under both N_2 and CO_2. In the blank experiment, this increase is due to the hydrogen evolution reaction (HER), while the higher current density in the presence of CO_2 can be ascribed to the improved kinetics of CO_2 reduction, and the enhanced current represents its reduction to formate. In order to deeply understand the effect of microsphere morphology on the CO_2 electrocatalytic performance, Fig. 4b presents the linear sweep voltammetric (LSV) scans in CO_2-saturated 0.5 M $KHCO_3$ solution on four electrodes, i.e., SnO_2/GDE-30, SnO_2/GDE-70, SnO_2/GDE-86 and SnO_2/GDE-100, respectively, where the SnO_2/GDE-86 electrode can give the earliest onset potential (about −0.49 V vs. SHE) compared to other three electrodes. As shown in Fig. 4b, the catalytic activity is increased with increasing the content of ethanol in the synthetic solution from 30% to 70%, as indicated by positively moving of onset potential. The maximum current density reaches 18 mA cm^{-2} for SnO_2/GDE-70 electrode. Note that when the content of ethanol in the synthetic solution is continued to be increased, the size of microspheres is increased, and the morphology of SnO_2 is changed to an independent microsphere, as shown in Fig. 3(b) and (c). Such changes may contribute to the catalytic activity for CO_2 electroreduction, probably leading to the enhanced energy efficiency. It can be seen the SnO_2/GDE-86 electrode, which possesses HMS-SnO_2 morphology on the electrode surface, gives the most positive onset potential shift of the 80 mV compared to SnO_2/GDE-30, and 60 mV compared to SnO_2/GDE-70. In addition, on the cathodic end of the curves, the maximum current density reaches to 17 mA cm^{-2} at the same time. When the content of ethanol in the synthetic solution is further increased (SnO_2/GDE-100 electrode), the performance for CO_2 reduction is decreased sharply with a current density of 13.4 mA cm^{-2} maintained, and a more negative onset potential of −0.56 V under the same conditions. As described in Fig. 3d, when the content of ethanol is increased to 100% while maintaining other synthesis condition unchanged, some microspheres structure is destroyed and the solid nanoparticle aggregates are appeared around SnO_2 microspheres. The decreased catalytic activity of SnO_2/GDE-100 might be partly caused by the destroyed HMS-SnO_2 structure [32].

3.3. Faradaic efficiency for electrochemical reduction of CO_2 to formate

Controlled potential electrolysis was performed to investigate the effect of applied potentials on Faradaic efficiencies for formate production at HMS-SnO_2 electrode. Electrolysis experiments were controlled in a range from −1.1 to −1.9 V vs. SHE in CO_2-saturated 0.5 M $KHCO_3$ solution, and the results are shown in Fig. 5a. The SnO_2/GDE-86 electrode with the best catalytic activity is selected as the target electrode. As reported in earlier reports [33], formate was observed as the dominant soluble product at negative potentials. In our experiments, it is observed that the production of formate on the HMS-SnO_2 electrode is strongly dependent on the electrode potential. After −1.1 V, the formate is started to be produced, and the amount of formate reached to 62.8 mg L^{-1}. With further decreasing the cathode potential from −1.1 to −1.9 V vs. SHE, both the current density and the amount of formate are increased. As shown in Fig. 5a, the SnO_2/GDE-86

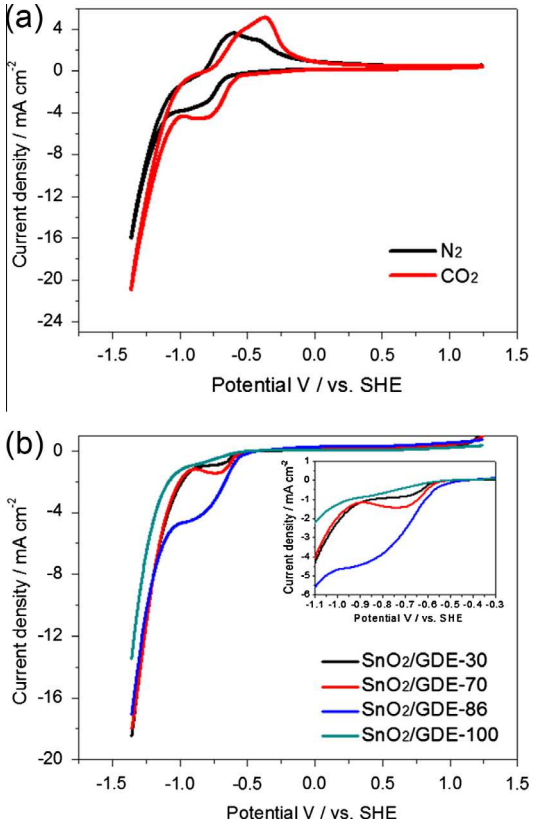

Fig. 4. (a) cyclic voltammetry (CV) curves of SnO_2/GDE-86 in N_2- and CO_2-saturated 0.5 M $KHCO_3$ electrolytes, and (b) Linear sweep voltammetric (LSV) of SnO_2/GDE-30, SnO_2/GDE-70, SnO_2/GDE-86 and SnO_2/GDE-100, scanning at 5 mV/s in CO_2-saturated 0.5 M $KHCO_3$.

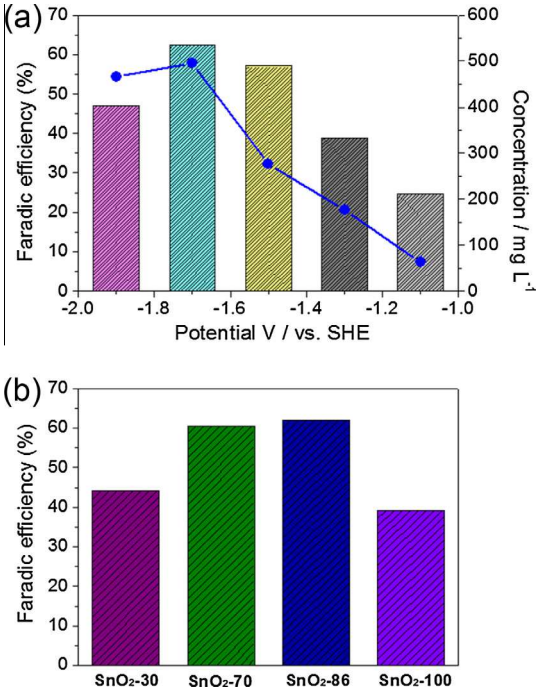

Fig. 5. (a) Formate production and faradaic efficiency of SnO_2/GDE-86 electrode with different potentials on different electrodes and (b) Faradaic efficiency of SnO_2 prepared from different proportions of ethanol to distilled water as solvent. Electrolysis time: 1 h.

Please cite this article in press as: Fu Y et al. Novel hierarchical SnO_2 microsphere catalyst coated on gas diffusion electrode for enhancing energy efficiency of CO_2 reduction to formate fuel. Appl Energy (2016), http://dx.doi.org/10.1016/j.apenergy.2016.03.115

electrode shows formate production range from 60 to 500 mg L^{-1}, reaching to a maximum at −1.7 V vs. SHE, and it is almost 6.5 times of that at a potential of −1.1 V. When the electrolysis potential is further decreased, the trend of the formate production shows a slight drop. Furthermore, Fig. 5a shows the Faradaic efficiencies for formate production as a function of electrode potential during the electrolysis process. The trends shown in Fig. 5a for the Faradaic efficiency as a function of potential are in an agreement with those reported for pure Sn metal electrodes [11,34–36]. It can be seen that the Faradaic efficiency for formate is increased when increasing the cathode potential from −1.1 V to −1.7 V, where it reaches to the maximum with a Faradaic efficiency of 62% at current density of 12.5 mA cm^{-2}. This value is a relatively high Faradaic efficiency when compared to previous reports as seen in Table S2. As the potential is decreased further, the Faradaic efficiency begins to drop. This may be caused by hydrogen evolution at very negative potentials [28,37,38]. This hydrogen evolution could compete with CO_2 reduction under these conditions, which can be observed by a large amount of hydrogen bubbles on the electrode surface. In order to deeply understand the effects of proportions of the ethanol to distilled water as a solvent on the catalysts' selectivity, the produced formate was determined and analyzed by ion chromatography (IC), after applying a constant potential of −1.7 V vs. SHE in a CO_2-saturated 0.5 M $KHCO_3$ electrolyte for 60 min. From Fig. 5b, it can be seen the highest Faradaic efficiency obtained in this work can be reached up to 62% for SnO_2/GDE-86 electrode. It is noted for the SnO_2/GDE-70 electrode, the Faradaic efficiency shows a similar value as SnO_2/GDE-86, indicating the integrated microsphere structure has a large effect on the selectivity of SnO_2 catalyst. When a lower content (30%) of ethanol is present in the synthetic solution, the Faradaic efficiency is sharply decreased, where there is no formation of HMS-SnO_2 structure. However, when the amount of ethanol is extremely high such as 100%, the Faradaic efficiency for producing formate also shows some drop, to where some HMS-SnO_2 structure is broken into small aggregated particles. This further demonstrates the Faradaic efficiency for CO_2 electroreduction strongly depends on the surface structure such as morphology and size control of the catalysts as-prepared [22–24]. For a fair comparison, all detailed results of Faradaic efficiency and concentration of formate are presented in Table S1.

3.4. Effect of $KHCO_3$ electrolyte for electroreduction CO_2

It was reported the $KHCO_3$ electrolyte solution in the absence of CO_2 had some effect on formate production, and the Faradaic efficiency toward formate production could be 2.7% with Sn electrode [37]. Here, we did some measurements for investigating the effect of purging gas, CO_2 or N_2, and HCO_3^- on the Faradaic efficiency toward formate production on SnO_2-86/GDE electrode, and the results are shown in Fig. 6. In 0.5 M $KHCO_3$ electrolyte with nitrogen bubbling, some formate was detected with IC. The Faradaic efficiency of formate reached to 2.4% and the concentration reached to13.2 mg L^{-1}. It should be pointed out that some amount of formate was also observed when purging with nitrogen in 0.5 M $KHCO_3$ electrolyte solution, which could be attributed to the electrochemical reduction of CO_2 derived from HCO_3^- due to the homogenous acid-baseReaction (1), the produced CO_2 is then reduced through Reaction (2)to produce formate along with the hydrogen evolution reaction (HER, Reaction (3)) [29,39].

$$HCO_3^- \leftrightarrow OH^- + CO_2 \quad (1)$$

$$CO_2 + H^+ + 2HCOO^- \quad E^o = -0.61 \text{ V vs. SHE} \quad (2)$$

$$2H^+ + 2H_2 \quad E^o = 0 \text{ V vs. SHE} \quad (3)$$

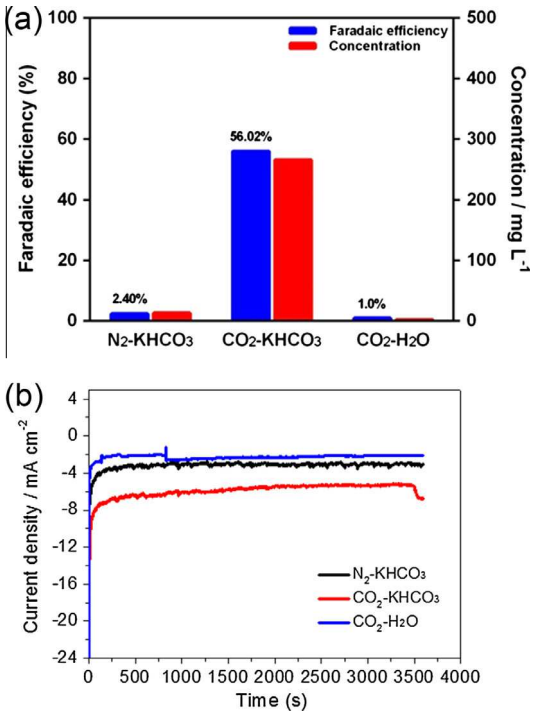

Fig. 6. (a) Faradaic efficiencies and concentrations of formate production and (b) the current density with electrolysis time for three electrolytes, i.e., N_2-$KHCO_3$, CO_2-$KHCO_3$ and CO_2-H_2O at −1.5 V vs. SHE. Electrolysis time: 1 h.

As shown in Fig. 6a, upon the solution is saturated with CO_2, the Faradaic efficiency toward formate production is increased to 56.0% (at −1.5 V vs. SHE), and the formate production is reached to 260 mg L^{-1}, which is almost 20 times of that under N_2. Moreover, the current density for the reduction reaction is increased by 1.7 times when purging with CO_2 compared to N_2. A similar improvements in the Faradaic efficiency, from 2.4% to 56.0%, and for the current density, from 3.1 mA cm^{-2} to 5.4 mA cm^{-2}, can be observed when exchanging N_2 for CO_2 purging in 0.5 M $KHCO_3$ solution. When replacing $KHCO_3$ with H_2O for CO_2 purging, the Faradaic efficiency of formate is as low as 1.0%, and the corresponding formate production is only reached to 2.2 mg L^{-1}, which is lower than $KHCO_3$ electrolyte with N_2 purging, and the current density is as low as 2.0 mA cm^{-2}, as shown in Fig. 6b. When using H_2O as the electrolyte, it cannot provide sufficient ions for the mass transfer diffusion on the surface of electrode, where there are only a little of the hydrogen ions reacted with CO_2 to form formate. When the electrolyte is pure water saturated with CO_2, the equilibrium of $CO_{2(aq)}/HCO_3^-/CO_3^{2-}$ can give 99.7% of the dissolved CO_2 in the form of liquid CO_2, and only 0.3% in the form of carbonate. In this case, the concentration of HCO_3^- is too low to provide conductivity of the solution for formate production. On the contrary, in $KHCO_3$ electrolyte saturated with nitrogen, there are large amounts of HCO_3^- and small amounts of CO_3^{2-}, which does not have liquid CO_2, leading to a trace amount of formate production by the equilibrium between HCO_3^- and CO_2 [40,41]. When replacing N_2 with CO_2, large amounts of liquid CO_2 and HCO_3^- are saturated in the electrolyte solution, which can provide sufficient CO_2 to the electrode for reduction. $KHCO_3$ solution supplies the most availability of reactants for CO_2 reduction leading to a higher Faradaic efficiency at more negative potentials [16]. The highest reduction current density can be observed in 0.5 M $KHCO_3$ and is attributed to the equilibrium between HCO_3^- and CO_2, which provides sufficient local dissolved CO_2 to the interface between SnO_2/GDE-86 electrode and electrolyte for the reaction, benefiting from the large hierarchical SnO_2 microsphere structure.

Please cite this article in press as: Fu Y et al. Novel hierarchical SnO_2 microsphere catalyst coated on gas diffusion electrode for enhancing energy efficiency of CO_2 reduction to formate fuel. Appl Energy (2016), http://dx.doi.org/10.1016/j.apenergy.2016.03.115

3.5. Stability of HMS-SnO_2 modified GDE for CO_2 electroreduction

To test the catalyst's stability, SnO_2-86/GDE electrode with a hierarchical microsphere structure was used, and the electrochemical reduction of CO_2 was controlled at −1.7 vs. SHE. Fig. 7a shows the current density as a function of electrolysis time. It can be seen that the total reduction current density as high as 12.2 mA cm^{-2} can be achieved in 0.5 M $KHCO_3$. The current density on the electrode is decreased sharply in the initial stage of the reaction, indicating that there is an intermediate product generation along with the CO_2 reduction reaction occurring on the electrode at the initial stage. However, after that the current density remains almost unchanged. With the extension of time, the reduction reaches to a steady state in the electrolyte, implying that the nature of the cathodic reaction is not changed. In order to further demonstrate this point, we have taken a comparison of XPS spectra of the cathode before and after electrolysis. The atomic percentages of Sn $3d_{3/2}$ and Sn $3d_{5/2}$ peaks also exhibit the known characteristics of SnO_2. As shown in Fig. 7b, the high-resolution Sn3d XPS spectrum before electrolysis exhibits binding energies of 495.0 and 486.5 eV that can be assigned to $Sn3d_{3/2}$ and $Sn3d_{5/2}$ ionizations, respectively, and the ratio of Sn $3d_{3/2}$:Sn $3d_{5/2}$ is 39:61. These energies are consistent with Sn(IV) bound to oxygen in SnO_2. After electrolysis, the binding energies of Sn $3d_{3/2}$ and Sn $3d_{5/2}$ with a fluctuation of only 0.1–0.2, exhibit a Sn $3d_{3/2}$:Sn $3d_{5/2}$ ratio of 43:57 (Fig. 7c). This suggests there is no occurrence of Sn(IV) oxide to Sn(0) reduction, and the native SnO_2 layer should be stable under the reduction conditions [21]. During electrolysis, the current is sustained without decreasing for at least 12 h at a current density of 12 mA cm^{-2} (Fig. 7a), which shows the high durability of the SnO_2/GDE-86 electrode for CO_2 electroreduction.

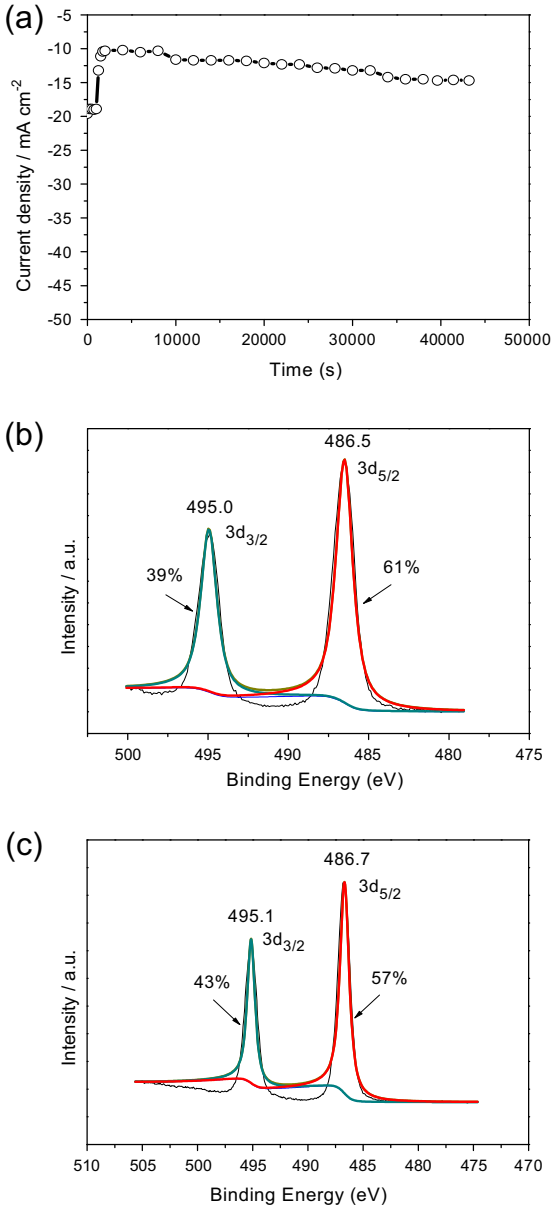

Fig. 7. (a) Stability, and High-resolution Sn 3d XPS spectra of micro-SnO_2 before (b) and after (c) electrolysis for 12 h during the electrochemical reduction of CO_2 in 0.5 M $KHCO_3$ solution at −1.7 V vs. SHE.

4. Conclusions

This work presents new experimental results on the development of micro-structured tin oxide catalysts coated GDE electrodes for CO_2 electroreduction in aqueous solution. The morphology- and size-controlled hierarchical tin oxide microspheres (HMS-SnO_2) are successfully synthesized using a hydrothermal self-assembled process, and employed as the cathode catalysts for CO_2 electroreduction to formate, a form of formate fuel, which can be transported readily or regenerated to electricity using fuel cells. Effects of different proportions of ethanol to distilled water in the synthetic solutions on the catalyst activity and selectivity are investigated. The results show that the catalytic activity is increased with increasing ethanol content from 30% to 86%, indicated by both the increased current density and positive onset potential. Among all electrodes studied, the SnO_2/GDE-86 electrode can give the most positive onset potential (about −0.49 V vs. SHE). This improvement is further demonstrated by the enhanced Faradaic efficiency observed during electrolysis experiments. The measurement results also show CO_2 reduction efficiencies on these HMS-SnO_2 catalysts are strongly dependent on the catalyst surface structure, size and the composition. The maximum Faradaic efficiency toward formate formation occurs on the SnO_2/GDE-86 electrode and can be as high as 62% at −1.7 V vs. SHE. In addition, the $KHCO_3$ electrolyte in the absence of CO_2 is found to show some contribution to the formate production. However, its Faradaic efficiency toward formate production is only 2.4%, which is attributed to the equilibrium between HCO_3^- and CO_2. The stability test indicates a high durability of the prepared HMS-SnO_2/GDE electrode with a stable current density (~12 mA cm^{-2}) over 12 h of continuous electrolysis operation. XPS spectra analysis demonstrates the SnO_2 layer is stable under the reduction conditions after a long time of electrolysis. The superior performance is credited to the morphology- and a size-controlled hierarchical structure, which may provide more active sites to accelerate the slow kinetics of the CO_2 reduction.

Acknowledgments

This work was financially supported by the National Natural Science Foundation of China (U1510120), the Project of Introducing Overseas Intelligence High Education of China (2016), the Innovation Program of the Shanghai Municipal Education Commission (14ZZ074), the International Academic Cooperation and Exchange Program of Shanghai Science and Technology Committee (14520721900) and the College of Environmental Science and Engineering, State Environmental Protection Engineering Center for Pollution Treatment and Control in Textile Industry, Donghua University. All the financial supports are gratefully acknowledged.

Appendix A. Supplementary material

Supplementary data associated with this article can be found, in the online version, at http://dx.doi.org/10.1016/j.apenergy.2016.03.115.

References

[1] Schrag DP. Preparing to capture carbon. Science 2007;315:812–3.
[2] Qiao JL, Liu YY, Hong F, Zhang JJ. A review of catalysts for the electroreduction of carbon dioxide to produce low-carbon fuels. Chem Soc Rev 2014;43:631–75.
[3] Jones JP, Prakash GKS, Olah GA. Electrochemical CO_2 reduction: recent advances and current trends. Isr J Chem 2014;54:1451–66.
[4] Alvarez-Guerra M, Albo J, Alvarez-Guerra E, Irabien A. Ionic liquids in the electrochemical valorisation of CO_2. Energy Environ Sci 2015;8:2574–99.
[5] Martin AJ, Larrazabal GO, Perez-Ramirez J. Towards sustainable fuels and chemicals through the electrochemical reduction of CO_2: lessons from water electrolysis. Green Chem 2015;17:5114–30.
[6] Albo J, Alvarez-Guerra M, Castaño P, Irabien A. Towards the electrochemical conversion of carbon dioxide into methanol. Green Chem 2015;17:2304–24.
[7] Olajire AA. Valorization of greenhouse carbon dioxide emissions into value-added products by catalytic processes. J CO_2 Util 2013;3–4:74–92.
[8] Sánchez-Sánchez CM, Montiel V, Tryk DA, Aldaz A, Fujishima A. Electrochemical approaches to alleviation of the problem of carbon dioxide accumulation. Pure Appl Chem 2001;73:1917–27.
[9] Kyriacou G, Anagnostopoulos A. Electroreduction of CO_2 on differently prepared copper electrodes – the influence of electrode treatment on the current efficiencies. J Electroanal Chem 1992;322:233–46.
[10] Wu JJ, Risalvato FG, Ma SG, Zhou XD. Electrochemical reduction of carbon dioxide III. The role of oxide layer thickness on the performance of Sn electrode in a full electrochemical cell. J Mater Chem A 2014;2:1647–51.
[11] Hori Y, Wakebe H, Tsukamoto T, Koga O. Electrocatalytic process of Co selectivity in electrochemical reduction of CO_2 at metal-electrodes in aqueous-media. Electrochim Acta 1994;39:1833–9.
[12] Yu XW, Pickup PG. Recent advances in direct formic acid fuel cells (DFAFC). J Power Sources 2008;182:124–32.
[13] Kang P, Zhang S, Meyer TJ, Brookhart M. Rapid selective electrocatalytic reduction of carbon dioxide to formate by an iridium pincer catalyst immobilized on carbon nanotube electrodes. Angew Chem Int Edit 2014;53:8709–13.
[14] Grasemann M, Laurenczy G. Formic acid as a hydrogen source – recent developments and future trends. Energy Environ Sci 2012;5:8171–81.
[15] Li H, Oloman C. Development of a continuous reactor for the electro-reduction of carbon dioxide to formate – part 2: scale-up. J Appl Electrochem 2007;37:1107–17.
[16] Wu JJ, Risalvato FG, Ke FS, Pellechia PJ, Zhou XD. Electrochemical reduction of carbon dioxide I. Effects of the electrolyte on the selectivity and activity with Sn electrode. J Electrochem Soc 2012;159:F353–9.
[17] Machunda RL, Ju H, Lee J. Electrocatalytic reduction of CO_2 gas at Sn based gas diffusion electrode. Curr Appl Phys 2011;11:986–8.
[18] Del Castillo A, Alvarez-Guerra M, Irabien A. Continuous electroreduction of CO_2 to formate using Sn gas diffusion electrodes. AIChE J 2014;60:3557–64.
[19] Koplјar D, Inan A, Vindayer P, Wagner N, Klemm E. Electrochemical reduction of CO_2 to formate at high current density using gas diffusion electrodes. J Appl Electrochem 2014;44:1107–16.
[20] Del Castillo A, Alvarez-Guerra M, Solla-Gullon J, Saez A, Montiel V, Irabien A. Electrocatalytic reduction of CO_2 to formate using particulate Sn electrodes: effect of metal loading and particle size. Appl Energy 2015;157:165–73.
[21] Chen Y, Kanan MW. Tin oxide dependence of the CO_2 reduction efficiency on tin electrodes and enhanced activity for tin/tin oxide thin-film catalysts. J Am Chem Soc 2012;134:1986–9.
[22] Qiao J, Jiang P, Liu J, Zhang J. Formation of Cu nanostructured electrode surfaces by an annealing-electroreduction procedure to achieve high-efficiency CO_2 electroreduction. Electrochem Commun 2014;38:8–11.
[23] Li CW, Kanan MW. CO_2 reduction at low overpotential on Cu electrodes resulting from the reduction of thick Cu_2O films. J Am Chem Soc 2012;134:7231–4.
[24] Tang W, Peterson AA, Varela AS, Jovanov ZP, Bech L, Durand WJ, et al. The importance of surface morphology in controlling the selectivity of polycrystalline copper for CO_2 electroreduction. Phys Chem Chem Phys 2012;14:76–81.
[25] Delacourt C, Ridgway PL, Kerr JB, Newman J. Design of an electrochemical cell making syngas ($CO + H_2$) from CO_2 and H_2O reduction at room temperature. J Electrochem Soc 2008;155:B42–9.
[26] Lee KR, Lim JH, Lee JK, Chun HS. Reduction of carbon dioxide in 3-dimensional gas diffusion electrodes. Korean J Chem Eng 1999;16:829–36.
[27] Lee J, Kwon Y, Machunda RL, Lee HJ. Electrocatalytic recycling of CO_2 and small organic molecules. Chem-Asian J 2009;4:1516–23.
[28] Prakash GKS, Viva FA, Olah GA. Electrochemical reduction of CO_2 over Sn-Nafion (R) coated electrode for a fuel-cell-like device. J Power Sources 2013;223:68–73.
[29] Lee S, Ocon JD, Son YI, Lee J. Alkaline CO_2 electrolysis toward selective and continuous $HCOO^-$ production over SnO_2 nanocatalysts. J Phys Chem C 2015;119:4884–90.
[30] Park MS, Wang GX, Kang YM, Wexler D, Dou SX, Liu HK. Preparation and electrochemical properties of SnO_2 nanowires for application in lithium-ion batteries. Angew Chem Int Edit 2007;46:750–3.
[31] Kapusta SD, Hackerman N. Anodic passivation of tin in slightly alkaline-solutions. Electrochim Acta 1980;25:1625–39.
[32] Zhang HX, Feng J, Zhang ML. Preparation of flower-like CuO by a simple chemical precipitation method and their application as electrode materials for capacitor. Mater Res Bull 2008;43:3221–6.
[33] Ohkawa K, Hashimoto K, Fujishima A, Noguchi Y, Nakayama S. Electrochemical reduction of carbon-dioxide on hydrogen-storing materials. 1. The effect of hydrogen absorption on the electrochemical-behavior on palladium electrodes. J Electroanal Chem 1993;345:445–56.
[34] Azuma M, Hashimoto K, Hiramoto M, Watanabe M, Sakata T. Electrochemical reduction of carbon-dioxide on various metal-electrodes in low-temperature aqueous $KHCO_3$ media. J Electrochem Soc 1990;137:1772–8.
[35] Hori Y, Kikuchi K, Suzuki S. Production of CO and CH_4 in electrochemical reduction of CO_2 at metal-electrodes in aqueous hydrogencarbonate solution. Chem Lett 1985:1695–8.
[36] Noda H, Ikeda S, Oda Y, Imai K, Maeda M, Ito K. Electrochemical reduction of carbon-dioxide at various metal-electrodes in aqueous potassium hydrogen carbonate solution. B Chem Soc Jpn 1990;63:2459–62.
[37] Köleli F, Atilan T, Palamut N, Gizir AM, Aydin R, Hamann CH. Electrochemical reduction of CO_2 at Pb- and Sn-electrodes in a fixed-bed reactor in aqueous K_2CO_3 and $KHCO_3$ media. J Appl Electrochem 2003;33:447–50.
[38] Jitaru M, Lowy DA, Toma M, Toma BC, Oniciu L. Electrochemical reduction of carbon dioxide on flat metallic cathodes. J Appl Electrochem 1997;27:875–89.
[39] Dutta A, Kuzume A, Rahaman M, Vesztergom S, Broekmann P. Monitoring the chemical state of catalysts for CO_2 electroreduction: an in operando study. ACS Catal 2015;5:7498–502.
[40] Kortlever R, Tan KH, Kwon Y, Koper MTM. Electrochemical carbon dioxide and bicarbonate reduction on copper in weakly alkaline media. J Solid State Electr 2013;17:1843–9.
[41] Sreekanth N, Phani KL. Selective reduction of CO_2 to formate through bicarbonate reduction on metal electrodes: new insights gained from SG/TC mode of SECM. Chem Commun 2014;50:11143–6.

Please cite this article in press as: Fu Y et al. Novel hierarchical SnO_2 microsphere catalyst coated on gas diffusion electrode for enhancing energy efficiency of CO_2 reduction to formate fuel. Appl Energy (2016), http://dx.doi.org/10.1016/j.apenergy.2016.03.115